Industrial Robot Permanent Magnet Synchronous Motor (PMSM) Application and Simulation

1st Guo Shiping
NUS ECE Master student
Singapore, Singapore
e0973856@u.nus.edu

1st Zeng Ruijie
NUS ECE Master student
Singapore, Singapore
zeng_ruijie@u.nus.edu

***Abstract*—This report investigates the performance of a Permanent Magnet Synchronous Motor (PMSM) in industrial robot position control. Dynamic and steady-state equations are derived and simulated in Jupyter Notebook, showcasing key motor characteristics. The analysis includes a focus on Maximum Torque per Ampere (MPTA) and effectiveness. The report further explores position control using Proportional-Integral-Derivative (PID) and Linear Quadratic Regulator (LQR) methods, presenting a comprehensive comparison of results. In conclusion, the report offers valuable insights into the exceptional performance and reliability of PMSM in industrial robot position control.**

***Index Terms*—Instrial Robot, PMSM, Position control, PI, LQR, Jupyter notebook**

I. Introduction

In robotics, motor performance is pivotal for precision and efficacy. Permanent Magnet Synchronous Motors (PMSMs) stand out for their efficiency, precise control, and high power density. Using permanent magnets for magnetic fields, PMSMs ensure synchronous stator-rotor rotation, making them ideal for precision-focused applications.

This research aims to create a comprehensive PMSM motor model for integration into a robot's control system. The focus is on understanding PMSM behavior, exploring control strategies, and assessing their applicability in diverse robotic tasks. The model serves to optimize robotic system performance.

The first section presents the mathematical derivatives of the model under stator and rotor coordinates, comparing the results obtained under these two coordinates. Subsequently, we conduct simulations for Maximum Torque per Ampere to analyze motor characteristics. Moving forward, we delve into position control simulations using PID and LQR methods, comparing their performance. Finally, a succinct analysis of power and efficiency concludes the report.

II. Define PMSM model

A. PMSM model Rotor coordinates [1]

This model is for machine in rotor coordinates. For simplicity we will assume $l_d = l_q$, which is the case with most surface-mounted permanent magnets on rotor. The mathematical equation of PMSM is generally on the d-q axis coordinate system. This conclusion is mainly on account of the theory of coordinate transformation.

The rotor lacks electromagnetic dynamics since the flux is generated by permanent magnets. Consequently, the dynamics

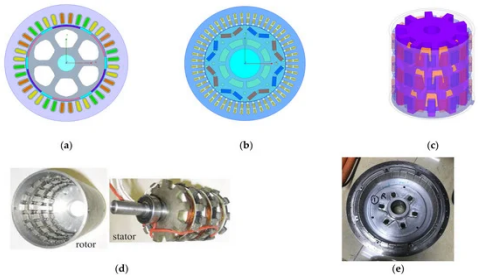

Fig. 1. Prototypes of the PMSM: (a) surface-mounted PMSM; (b) interior PMSM; (c) claw-pole PMSM; (d) transverse flux PMSM; (e) axial flux PMSM.

in the d-q frame are primarily described by the stator voltage equation. The presence of saliency influences the flux linkages in this context. Baed on fig2 we can easily get the voltage

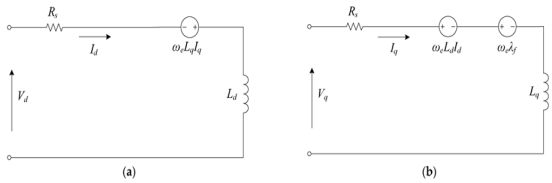

Fig. 2. Equivalent circuit.

equations. The V_d voltage can be expressed as (The meaning of these variables can refer to the Table1)

$$\vec{v}_s^F = \vec{i}_s^F r_s - j w_s \psi_s^F + \frac{d\vec{\psi}_s^F}{d\tau} \tag{1}$$

$$\vec{v}_{sd} = \vec{i}_{sd} r_s - w_s \psi_{sq} + \frac{d\psi_{sd}}{d\tau} \tag{2}$$

$$\vec{v}_{sd} = \vec{i}_{sd} r_s - w_s l_q i_{sq} + l_d \frac{di_{sd}}{d\tau} \tag{3}$$

The V_q voltage can be expressed as

$$\vec{v}_{sq} = \vec{i}_{sq} r_s + w_s \psi_{sd} + \frac{d\psi_{sq}}{d\tau} \tag{4}$$

$$\vec{v}_{sq} = \vec{i}_{sq} r_s + w_s l_q i_{sq} + w_s \psi_{r,m} + l_q \frac{di_{sq}}{d\tau} \tag{5}$$

The PMSM mathematical model employs a disassembled representation of variables, significantly simplifying the complexity of the model. This disassembly allows for individual

control of torque components. Consequently, the state-space dynamic model can be further simplified:

$$\frac{di_{sd}}{d\tau} = -\frac{r_s}{l_d} i_{sd} + w_s \frac{l_q}{l_d} i_{sq} + \frac{v_{sd}}{l_d} \tag{6}$$

$$\frac{di_{sq}}{d\tau} = -\frac{r_s}{l_q} i_{sq} - w_s \frac{l_d}{l_q} i_{sd} - w_s \frac{\psi_{r,m}}{l_q} + \frac{v_{sq}}{l_q} \tag{7}$$

$$m_e = \vec{\psi_s} \times \vec{i_s} = \Im[\vec{\psi_s}^* \vec{i_s}] \tag{8}$$

$$= \psi_{r,m} i_{sq} + (l_d - l_q) i_{sd} i_{sq} \tag{9}$$

$$\frac{dw}{d\tau} = \frac{m_e - m_L}{\tau_m} \tag{10}$$

B. PMSM model in Stator coordinates [2]

Employing the dq coordinate dynamic model simulation is a commonly adopted and relatively straightforward method for studying dynamic systems. In our efforts to gain a deeper understanding of the PMSM and help us study this course we ventured into modeling in stator coordinates.

To obtain the mathematical equation of the PMSM on the stationary axis coordinate system, it is only necessary to transform the equation on the d-q axis coordinate system to the $\alpha - \beta$ axis coordinate system using inverse Park. Therefore, the voltage equation in the $\alpha - \beta$ coordinate system can be expressed as(assume $l_d = l_q = l_s$)

$$\vec{v_s} = r_s \vec{i_s} + l_s \frac{d\vec{i_s}}{d\tau} + \frac{d\vec{\psi}_{r,m}}{d\tau} \tag{11}$$

$$\vec{\psi}_{r,m} = |\psi_{r,m}| e^{j\delta} = \psi_{r,m\alpha} + j\psi_{r,m\beta} \tag{12}$$

$$\vec{v_s} = r_s \vec{i_s} + l_s \frac{d\vec{i_s}}{d\tau} + j w_s \vec{\psi}_{r,m} \tag{13}$$

$$v_{s\alpha} = r_s i_{s\alpha} + l_s \frac{di_{s\alpha}}{d\tau} - w_s \psi_{r,m\beta} \tag{14}$$

$$v_{s\beta} = r_s i_{s\beta} + l_s \frac{di_{s\beta}}{d\tau} + w_s \psi_{r,m\alpha} \tag{15}$$

For current

$$\frac{di_{sa}}{d\tau} = -\frac{r_s}{l_s} i_{sa} + \frac{v_{sa}}{l_s} - \frac{d\psi_a}{l_s dt} \tag{16}$$

$$\frac{di_{sb}}{d\tau} = -\frac{r_s}{l_s} i_{sb} + \frac{v_{sb}}{l_s} - \frac{d\psi_b}{l_s dt} \tag{17}$$

C. Steady state model

For steady state $\frac{dw}{d\tau} = 0, \frac{di_{sd}}{d\tau} = 0, \frac{di_sq}{d\tau} = 0$

$$\vec{v}_{sd} = \vec{i}_{sd} r_s - w_s \psi_{sd} \tag{18}$$

$$\vec{v}_{sd} = \vec{i}_{sd} r_s - w_s l_q i_{sq} \tag{19}$$

$$\vec{v}_{sq} = \vec{i}_{sq} r_s + w_s \psi_{sd} \tag{20}$$

$$\vec{v}_{sq} = \vec{i}_{sq} r_s + w_s l_d i_{sd} + w_s \psi_{r,m} \tag{21}$$

III. Simulation

Before embarking on PMSM position control, it is essential to explore key features of the motor, including both dynamic and steady-state characteristics. Subsequent to this analysis, the design of control strategies can be tailored to the dynamic system's behavior, ensuring an effective and well-matched approach to position control.

TABLE I
VARIABLES

v_{sd}	Stator voltage in d ax direction
v_{sq}	Stator voltage in q ax direction
$v_{s\alpha}$	Stator voltage in α direction
$v_{s\beta}$	Stator voltage in β direction
i_{sd}	Stator current in d direction
i_{sq}	Stator current in q direction
$i_{s\alpha}$	Stator current in α direction
$i_{s\beta}$	Stator current in β direction
ψ_{sd}	Stator flux component
ψ_{sq}	Stator flux component
$\psi_{s\alpha}$	Stator flux component
$\psi_{s\beta}$	Stator flux component
l_d	Stator inductance in d ax direction
l_q	Stator inductance in q ax direction
l_s	Stator inductance
w_s	Electrical angular velocity of the sub
r_s	Stator phase resistance
$\psi_{r,m}$	Rotor flux linkage

TABLE II
MOTOR PARAMETERS

V_b	Rated voltage	220V
I_s	Rated current	16.7A
p	Pole pairs	4
r_s	Stator resistance	0.0426Ω
l_d	d-axis inductance(p/u)	2.33mH
l_q	q-axis inductance(p/u)	2.33Hm
τ_{mech}	Mechanical time constant	100
$\psi_{r,m}$	Rotor flux linkage	0.9Wb

A. Steady state model

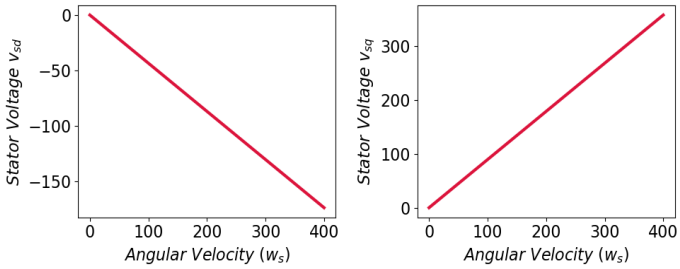

Fig. 3. Steady state current and voltage

In steady state, the torque is consistent. In order to achieve this, the i_q and i_d changes proportionally when the w_s increases. The i_q is the dominant factor to control output torque. The i_d changes with the changing of w_s to generate the magnetic field and interacts with the permanent magnet field. So, we can see the final output is consistent torque.

B. Current control

We adhered to the structure outlined in Figure 5, where we initiated the process by providing a reference current. Subsequently, employing PI control, we derived the voltage using Equation (1). This approach resulted in two distinct circles—the current control circle and the voltage control

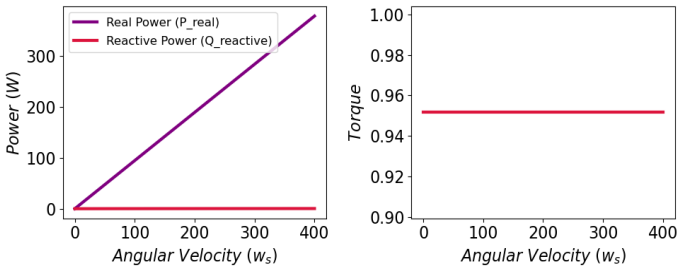

Fig. 4. Steady state power and torque

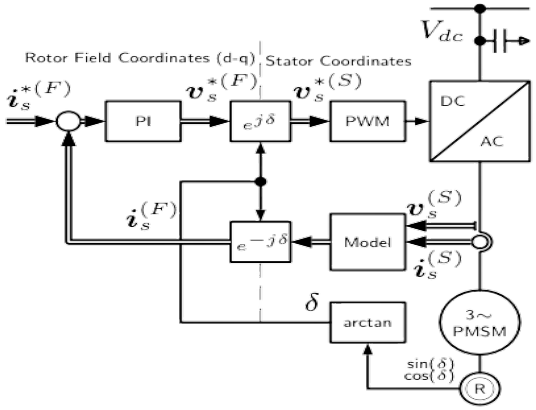

Fig. 5. Current control

circle—both contributing to the realization of current control. To streamline the process, we opted not to apply PWM control, and instead, directly utilized coordinate transformation along with equations (3), (5), (6), and (7) to complete the control loop. The current control results can refer to the figure 6. The results is good.

C. Dynamic simulation

Initially, we conducted current control simulations for PMSM with a symmetrical rotor. Given the real-world scenario where the direct ld and quadrature inductances lq are closely matched, we made the assumption ld=lq and proceeded with the following simulations.

The simulation commenced with an initial current of 0 and an initial rotational velocity of -5 rad/s. The first step involved a change in the current lq to 0.8 for a specific duration, followed by a subsequent change to -0.35.

The figures are easily interpretable: the rotational speed initiates from -0.5 and progressively accelerates, reversing direction as per the current input. The absence of initial current dynamics is noteworthy, with a smooth and slightly overshooting current initiation. Crucially, the output torque and rotational speed exhibit seamless transitions without significant overshooting or oscillations.

When comparing the $\alpha - \beta$ coordinate model with the $d - q$ coordinate model, it becomes evident that achieving current or voltage control in the $\alpha - \beta$ coordinate system is more challenging. Conversely, the $d - q$ coordinate method

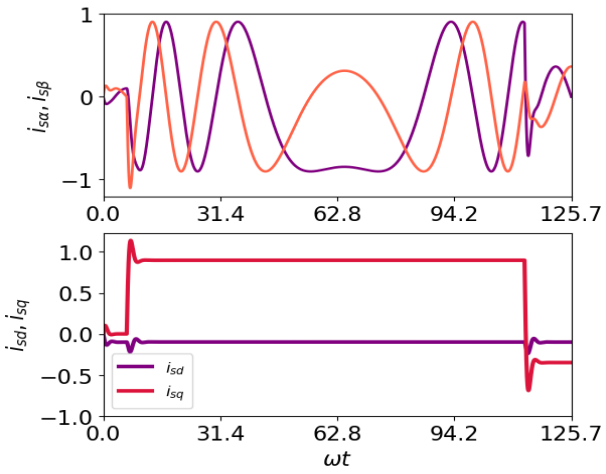

Fig. 6. Dynamic current

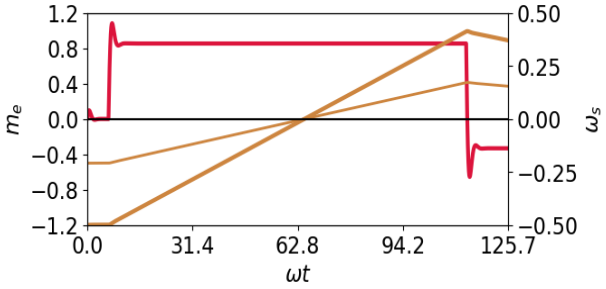

Fig. 7. Dynamic torque and w

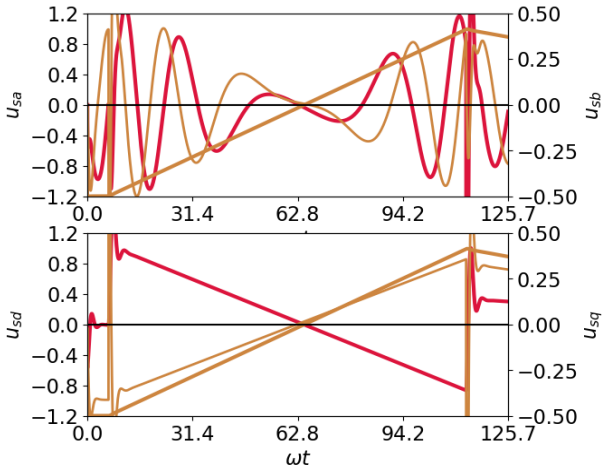

Fig. 8. Dynamic voltage

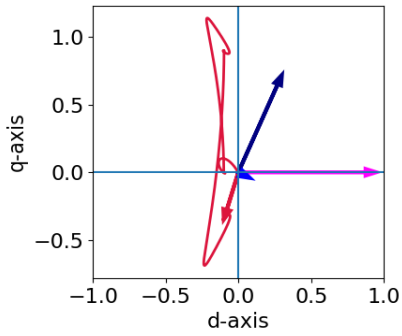

Fig. 9. Current trajectory

proves to be much more straightforward for accomplishing precise current control. That's the biggest advantage of $d-q$ coordinate model approach.

In the current trajectory, a notable distinction is observed between the d-axis and q-axis currents. Notably, the q-axis current undergoes more significant changes, underscoring its primary role in torque control. This observation reinforces the understanding that q-axis current is the main contributor to torque regulation.

D. $l_d \neq l_q$ situation

Up to now, all the simulations are based on $l_q = l_d$ situation. We also test the other situations.

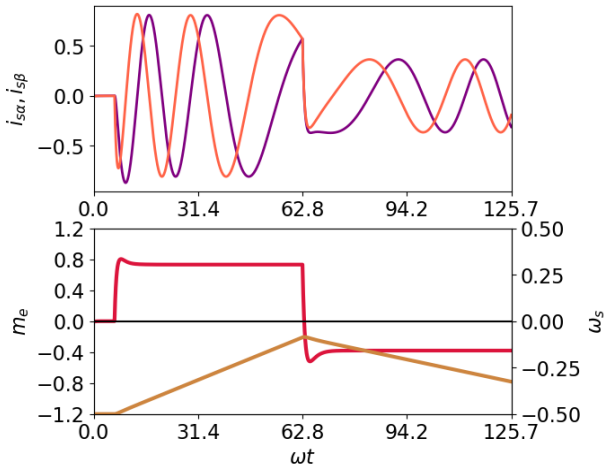

Fig. 10. $l_d < l_q$ simulation result

Figures 10 and 11 depict two scenarios with identical parameters, differing only in the values of l_d and l_q. From the results, a clear similarity emerges: both situations demonstrate effective control of current and rotation speed. The primary distinction lies in the rotational acceleration. Specifically, a larger Ld results in a more robust field along the d-axis, augmenting the motor's torque production capacity. Consequently, when $l_d > l_q$, the torque notably increase faster compared to the scenario with$l_d < l_q$.

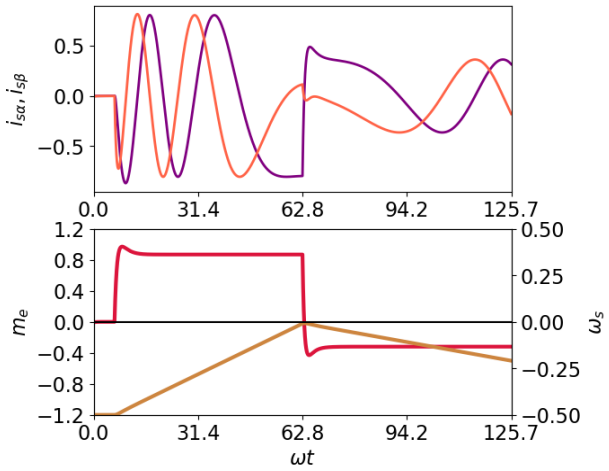

Fig. 11. $l_d > l_q$ simulation result

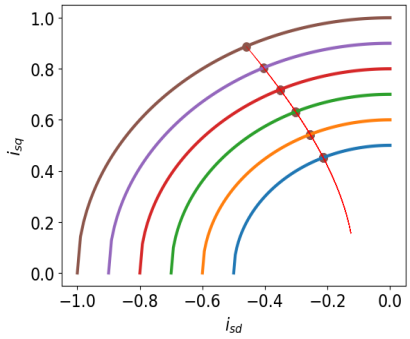

Fig. 12. MPTA

E. Maximum Torque per Ampere(MPTA)

MPTA analysis in a PMSM optimizes efficiency, current utilization, and dynamic performance by identifying the point for maximum torque per ampere. This enhances motor operation efficiency and provides insights for designing control strategies in robot position control.

The simulation reveals that the maximum torque position is not linearly related to id and iq. In practical applications, striving to align with the MPTA point becomes essential to improve the overall efficiency of robot operations.

IV. Position Control

Position control is the most important part for robot movement control. In order achieve precise position control My partner mainly focuses on the PID control method and I focus on LQR [3] method. In the end, we compare our results and do some analysis.

A. Control Modeling

The dynamic model of the PMSM described by equations (6) to (10) is inherently nonlinear due to cross-coupling effects. Linearization, detailed in [4], involves defining new variables,

especially when magnetic symmetry is present in the motor, resulting in equal inductances in the d and q axes.

$$l = l_d = l_q \tag{22}$$
$$v_d = -lw_r i_q \tag{23}$$
$$v_q = lw_r i_d \tag{24}$$

the linearized dynamic model of PMSM takes the form of following equations:

$$\frac{di_d}{dt} = \frac{v_d}{l} - \frac{r_s i_d}{l} \tag{25}$$
$$\frac{di_1}{dt} = \frac{v_1}{l} - \frac{r_s i_1}{l} - \frac{w_r}{l} \tag{26}$$

Equations (25) and (26) reveal that the dynamical model of the PMSM has been successfully decoupled. The current in the d-axis now solely relates to variables in the d-axis, mirroring a similar case in the mechanical model presented by the following two equations:

$$\frac{dw_r}{dt} = \frac{m_{meth} - m_l}{\tau_{meth}} \tag{27}$$
$$\frac{d\theta}{dt} = w_r \tag{28}$$

Combine all the equations above we can form a continous state-spcae model for PMSM as follows:

$$\dot{x} = Ax + Bu \tag{29}$$
$$x = [i_q,\ i_d,\ w_r]^T \tag{30}$$

u is the input vector which is given by

$$u = [v_q v_d]^T \tag{31}$$

Matrices A and B of the state space model can be described as follows:

$$A = \begin{bmatrix} \frac{r_s}{l} & 0 & \frac{P}{l} \\ 0 & \frac{r_s}{l} & 0 \\ \frac{1.5P}{l} & 0 & 0 \end{bmatrix}$$
$$B = \begin{bmatrix} \frac{1}{l} & 0 \\ 0 & \frac{1}{l} \\ 0 & 0 \end{bmatrix} \tag{32}$$

The vector control method, rooted in field orientation, is consistently employed for PMSM. Specifically, we utilize a method that necessitates keeping i_d [5], ensuring the stator current vector aligns with the q-axis. This alignment results in the electromagnetic torque being linearly proportional to the q-axis current, a value determined through closed-loop control. While straightforward, this approach offers high dynamic performance. Consequently, the state-space dynamic model of the PMSM can be further simplified. For a detailed explanation, please refer to the following description.

$$\dot{x} = Ax + Bu + w$$
$$y = Cx \tag{33}$$

$$x = [i_1,\ ,w_r,\ \theta_r]^T, u = v_q, w = T_l \tag{34}$$

$$A = \begin{bmatrix} \frac{r_s}{l} & -\frac{P}{l} & 0 \\ \frac{1.5P}{l} & 0 & 0 \\ 0 & 1 & 0 \end{bmatrix}$$
$$B = \begin{bmatrix} \frac{1}{l} \\ 0 \\ 0 \end{bmatrix} \tag{35}$$

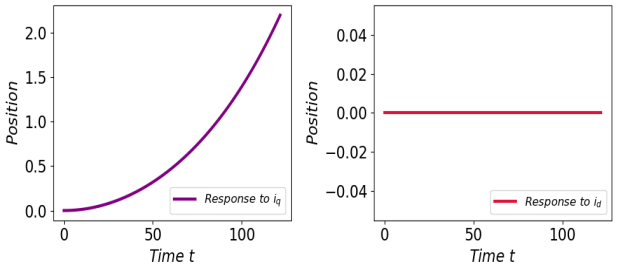

Fig. 13. Open loop response

The most challenging part for LQR is how to design the weight matrix Q and R, here I test the following parameters and check the results

$$Q = identity(\begin{bmatrix} 0.1 & 15 & 0.1 \end{bmatrix})$$
$$R = idendity(\begin{bmatrix} 10 & 1 \end{bmatrix}) \tag{36}$$

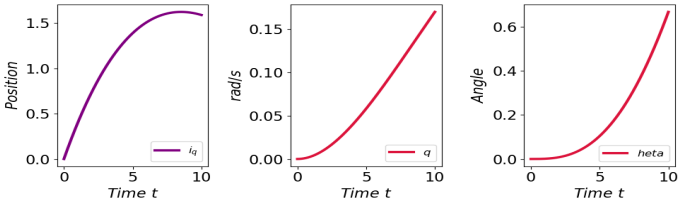

Fig. 14. Discrate time LQR feedback control

We can see the LQR works, but this is not enough to achieve precise position control because in practice the disturbance is unavoidable and precise and fast reponse is very cruical for robot. So, augmented matrix control is used.

B. Augmented matrix control

Let

$$\dot{x}_I = y - r = x_1 - r \tag{37}$$

Add in original state space model

$$\begin{bmatrix} \dot{i_q} \\ w_r \\ \theta_r \\ x_I \end{bmatrix} = \begin{bmatrix} 0 & 1 & 0 & 0 \\ -1.2 & -3.71 & 0 & 0 \\ 1 & 0 & 0 & 0 \\ 0 & 0 & 1 & 0 \end{bmatrix} \begin{bmatrix} i_q \\ w_r \\ \theta_r \\ x_I \end{bmatrix} + \begin{bmatrix} \frac{1}{l} \\ 0 \\ 0 \\ 0 \end{bmatrix} u + \begin{bmatrix} 0 \\ 0 \\ -1 \\ 0 \end{bmatrix} r + \begin{bmatrix} 0 \\ 1 \\ 0 \\ 0 \end{bmatrix} v$$

$$y = \begin{bmatrix} 0 & 0 & 1 & 0 \end{bmatrix} \begin{bmatrix} i_q \\ w_r \\ \theta_r \\ x_I \end{bmatrix} \tag{38}$$

The parameters I choose are

$$A = \begin{bmatrix} 0.001 & 0 & 0 & 0 \\ 0 & 100000 & 0 & 0 \\ 0 & 0 & 10000000 & 0 \\ 0 & 0 & 0 & 1 \end{bmatrix} \quad (39)$$
$$B = 0.00001$$

The simulation results are

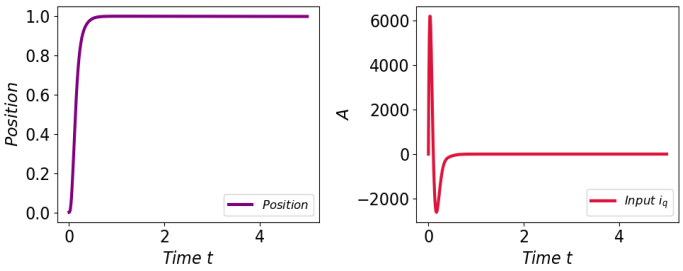

Fig. 15. LQR high performance position control result

The position control results are favorable, exhibiting rapid and precise responses. However, the challenge lies in the impractically high peak current values exceeding 6000, necessitating further parameter adjustments. Despite this, the efficacy of LQR control strategy is apparent, demonstrating optimal control outcomes need high requirement of inputs. The new parameters are

$$A = \begin{bmatrix} 0.1 & 0 & 0 & 0 \\ 0 & 40000 & 0 & 0 \\ 0 & 0 & 100000 & 0 \\ 0 & 0 & 0 & 1 \end{bmatrix} \quad (40)$$
$$B = 0.1$$

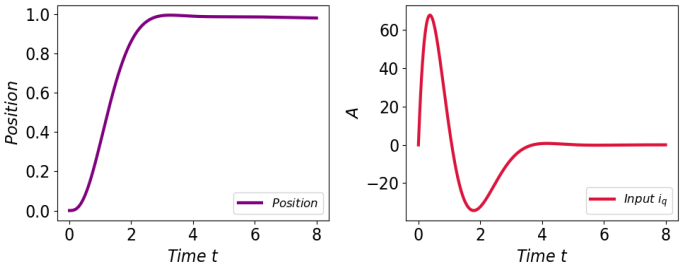

Fig. 16. LQR position control result

C. Compare

With the introduction of new parameters for Q and R, the results remain commendable, reinforcing the observation that, in comparison to PI control, LQR is a superior choice. While PI control exhibits a faster response, it is plagued by overshooting, detrimentally impacting robot performance. In contrast, although LQR still yields higher input values, these currents are readily achievable in practical industrial settings. We can also choose other parameters to make the input down Actually, we also want to design a disturbance rejection LQR controller, but the result is not ideal and need further research.

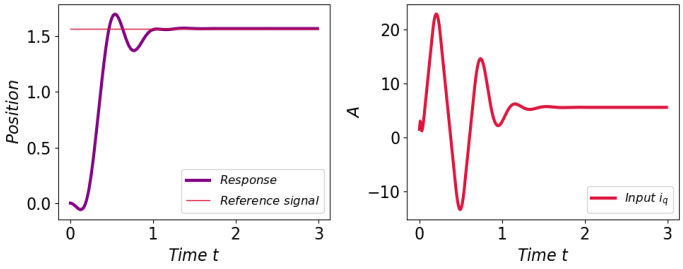

Fig. 17. PID control result

V. Power Analysis

The model has undergone significant simplification, we do a basic power analysis. The power consumption is depicted

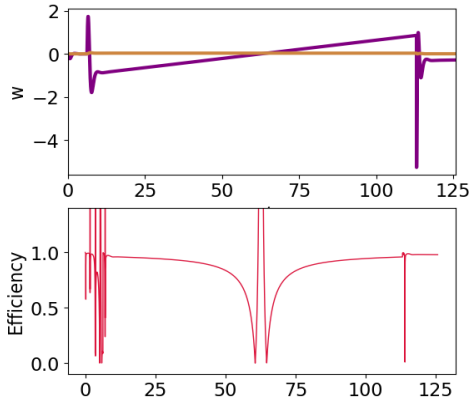

Fig. 18. Power analysis

in Figure 18, with accompanying efficiency curves. Notably, the efficiency remains consistently high, nearing 1 in most conditions. However, noteworthy fluctuations are observed when the current or rotor changes direction, signaling areas of consideration in practical applications. These fluctuations warrant attention in real-world scenarios.

VI. Conclusion

My partner and I successfully simulated the PMSM model, enhancing our theoretical understanding. In future work, we aim to explore advanced control methods and compare them with other motor types.

References

[1] Electric Motor Drives, R Krishnan Pearson International.

[2] Yi Song and Zehang Song and Xiaodong Yao, Permanent Magnet Synchronous Motor Control Based on New Sliding Mode Observer, Journal of Physics: Conference Series, volum 2218, pages 12-58, 2022

[3] Wen-Jun Xu,Permanent Magnet Synchronous Motor with Linear QuadraticSpeed Controller, Energy Procedia, Volume 14, 2012, Pages 364-369, ISSN 1876-6102.

[4] L.M. Grzesiak, T. Tarczewski, Permanent magnet synchronous servo-drive with state position controller, 13th Power Electronics and Motion Control Conference. EPE-PEMC 2008, pp.1071-1076

[5] Y.P Xu, Y.R. Zhong, H.Yang, Research on vector control and direct torque control for permanent magnet synchronous motors, Power Electronics, vol.42, no.1, pp.60-62,2008.